

Hyperconcentration for multipartite entanglement via linear optics

Xihan Li^{1,2} and Shohini Ghose^{1,3}

¹Department of Physics and Computer Science, Wilfrid Laurier University, Waterloo, Canada N2L 3C5

² Department of Physics, Chongqing University, Chongqing, China 400044

³ Institute for Quantum Computing, University of Waterloo, Canada N2L 3G1

E-mail: xihanlicqu@gmail.com, sghose@wlu.ca

Abstract. We present a hyperconcentration scheme for nonlocal N -photon hyperentangled Greenberger-Horne-Zeilinger states. The maximally hyperentangled state, in which N particles are entangled simultaneously in the polarization and the spatial mode, can be obtained with a certain probability from two partially hyperentangled states. The hyperconcentration scheme is based on one polarization parity check measurement, one spatial mode parity check measurement and $N - 2$ single-photon two-qubit measurements. The concentration only requires linear optical elements, which makes it feasible and practical with current technology.

1. Introduction

Entanglement is an important resource in quantum information processing, and is widely used in quantum communication and computation, including quantum key distribution [1, 2, 3], quantum secret sharing [4], quantum dense coding [5], quantum teleportation [6], quantum secure direct communication [7, 8, 9], quantum repeater [10] and so on. Entanglement can be generated in different degrees of freedom (DOF) of physical entities such as photons, electrons, atoms, etc. Among these, the photon is an interesting candidate for quantum communication due to its manipulability and high-speed transmission. The photon has many DOFs to carry quantum information, such as spatial modes, time-bins, polarization, frequency, and orbital angular momentum. Besides the conventional entanglement in which photons are entangled in a single DOF, there is the possibility of hyperentanglement in which photons are entangled in more than one DOF [11, 12, 13]. Hyperentangled states can increase the capacity of quantum information processing since each photon carries more than one qubit [14, 15, 16, 17, 18, 19]. Moreover, hyperentanglement has some important applications in entanglement purification [20, 21, 22, 23, 24, 25] and state analysis [26, 27, 28, 29, 30, 31].

In most quantum communication schemes based on entanglement, maximal entanglement is required to ensure efficiency and security. However, maximal

entanglement is fragile and in practice, it is difficult to preserve during transmission and storage. The inevitable interaction with the environment degrades the fidelity and degree of entanglement of the quantum state, which subsequently affects the security and efficiency of quantum communication protocols. Many solutions have been proposed to recover high quality entangled states from polluted less-entangled samples. One example is entanglement concentration, which extracts a maximally entangled state from an ensemble of less-entangled pure states. The first entanglement concentration scheme was proposed in 1996 based on the Schmidt projection method [32]. Later, two entanglement concentration schemes based on entanglement swapping were proposed [33, 34]. In 2001, entanglement concentration schemes using linear optical elements were proposed and demonstrated [35, 36]. During the past few years, many interesting entanglement concentration schemes considering different physical systems, different entangled states and exploiting different components have been discussed in the literature [37, 38, 39, 40, 41, 42, 43]. These entanglement concentration schemes can be classified into two groups based on whether the parameters of the less-entangled states are known or not. If the parameters are unknown, an ensemble of less-entangled states is required to distill maximal entanglement. Otherwise, additional states can be prepared or optical elements can be manipulated according to the known parameters, to accomplish the concentration.

Since hyperentanglement has increasing applications in quantum information processing, the concentration of hyperentangled states has attracted much attention recently. In 2013, Ren *et al.* proposed two hyperentanglement concentration schemes for a two-photon four-qubit system, in which only linear optics was required [45]. They also proposed a hyperentanglement concentration scheme assisted by diamond NV centers inside photonic crystal cavities [46]. One of us also proposed two hyperconcentration schemes with known and unknown parameters, respectively [47]. Recently, a general hyperentanglement concentration was also proposed [48].

In this paper, we present the first hyperconcentration scheme for N -photon hyperentangled Greenberger-Horne-Zeilinger (GHZ) states, which are simultaneously entangled in both the polarization and spatial mode DOFs. The scheme uses two less-entangled states and the concentration is realized with linear optics elements only. After one polarization parity check measurement, one spatial mode parity check measurement and $N - 2$ single-photon measurements, the N parties share the maximally hyperentangled GHZ states with a certain probability. The scheme can be implemented across an N -party network, where the parties are remotely located and do not need to interact with each other. A notable point is that the hyperconcentration success probability does not decrease with the number of photons - it remains the same as the two-photon success probability. We also discuss possible sources of error and how to address them in a practical setting.

2. Parity check devices for different degrees of freedom

Before we demonstrate our hyperconcentration scheme, we introduce two parity check devices for the polarization and the spatial mode DOFs, respectively. These parity check devices are used to select the even-parity states in the given DOF and then measure one photon both in the polarization and the spatial mode DOFs. A schematic for

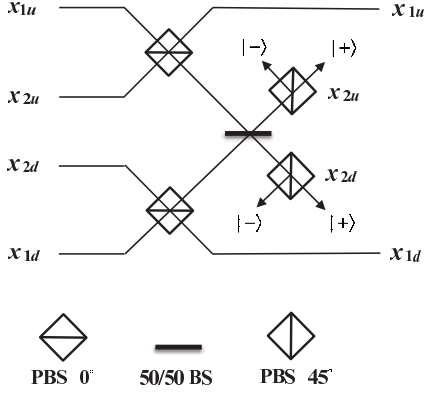


Figure 1. The schematic diagram of the polarization parity check device. The photon X_1 (X_2) enters the apparatus via two potential spatial modes x_{1u} and x_{1d} (x_{2u} and x_{2d}). The PBS oriented at 0° transmits the V state and reflects the H state. Then the photon in x_{2u} or x_{2d} is projected onto the diagonal basis of spatial modes by the beam splitter and then measured in the polarization diagonal basis $|\pm\rangle$ with the help of PBS at 45° , which transmits the $|+\rangle$ and reflects $|-\rangle$ state.

the polarization parity check (PPC) is shown in Fig.1. We start with four possible spatial modes for two input photons $1u, 1d, 2u$ and $2d$. We use two different kinds of polarizing beam splitters (PBS). The PBS oriented at 0° transmits the vertical polarization state $|V\rangle$ and reflects the horizontal one $|H\rangle$. The PBS at 45° transmits the $|+\rangle = \frac{1}{\sqrt{2}}(|H\rangle + |V\rangle)$ and reflects the $|-\rangle = \frac{1}{\sqrt{2}}(|H\rangle - |V\rangle)$. And the effect of the 50:50 beam splitter (BS) can be described as

$$In_u \rightarrow \frac{1}{\sqrt{2}}(Out_u + Out_d), \quad (1)$$

$$In_d \rightarrow \frac{1}{\sqrt{2}}(Out_u - Out_d). \quad (2)$$

Here In_u and In_d are the up and down input ports, while Out_u and Out_d are the two output ports of the BS. The PBS at 0° is used to compare the polarization parity of the two input photons. The BS is used to measure the spatial modes in the diagonal basis $|\pm'\rangle = \frac{1}{\sqrt{2}}(|u\rangle \pm |d\rangle)$ while the PBSs at 45° are utilized to measure the polarization in the diagonal basis $|\pm\rangle$. The evolution of different possible input states are

$$\begin{aligned} & |HH\rangle \otimes (|x_{1u}\rangle + |x_{1d}\rangle)(|x_{2u}\rangle + |x_{2d}\rangle) \\ \rightarrow & |HH\rangle \otimes (|x_{1u}x_{2u}\rangle + |x_{1u}x_{2d}\rangle + |x_{1d}x_{2u}\rangle + |x_{1d}x_{2d}\rangle), \end{aligned} \quad (3)$$

$$\begin{aligned} & |HV\rangle \otimes (|x_{1u}\rangle + |x_{1d}\rangle)(|x_{2u}\rangle + |x_{2d}\rangle) \\ \rightarrow & |HV\rangle \otimes (|x_{1u}x_{1u}\rangle + |x_{1u}x_{1d}\rangle + |x_{1d}x_{1u}\rangle + |x_{1d}x_{1d}\rangle), \end{aligned} \quad (4)$$

$$\begin{aligned}
& |VH\rangle \otimes (|x_{1u}\rangle + |x_{1d}\rangle)(|x_{2u}\rangle + |x_{2d}\rangle) \\
\rightarrow & |VH\rangle \otimes (|x_{2u}x_{2u}\rangle + |x_{2u}x_{2d}\rangle + |x_{2d}x_{2u}\rangle + |x_{2d}x_{2d}\rangle), \tag{5}
\end{aligned}$$

$$\begin{aligned}
& |VV\rangle \otimes (|x_{1u}\rangle + |x_{1d}\rangle)(|x_{2u}\rangle + |x_{2d}\rangle) \\
\rightarrow & |VV\rangle \otimes (|x_{2u}x_{1u}\rangle + |x_{2u}x_{1d}\rangle + |x_{2d}x_{1u}\rangle + |x_{2d}x_{1d}\rangle). \tag{6}
\end{aligned}$$

From the above expression, we find that for the odd-parity states $|HV\rangle$ or $|VH\rangle$, there are zero or two photons detected by these four detectors set up on paths x_{2u} and x_{2d} . However, for the even-parity polarization states $|HH\rangle$ or $|VV\rangle$, there is one and only one photon detected by these detectors in principle. Therefore, we can distinguish the parity of polarization states according to the detection in the output ports. With the help of a BS and the PBS oriented at 45° , the photon appearing at the output port 2 can be measured in the diagonal basis in both the polarization DOF and the spatial one.

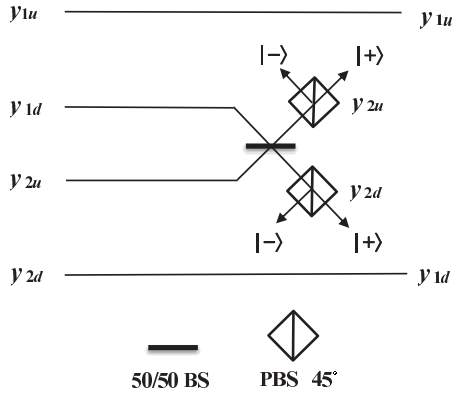


Figure 2. The schematic diagram of the spatial mode parity check device. The photon Y_1 (Y_2) enters the apparatus via the two potential spatial modes y_{1u} and y_{1d} (y_{2u} and y_{2d}). Photons in y_{1d} and y_{2u} interfere in the 50:50 beam splitter, after which the photons are measured in the polarization diagonal basis via the PBS at 45° . The name of y_{2d} is changed to y_{1d} for the selection purpose.

The schematic for the spatial mode parity check (SPC) is shown in Fig.2. It is used to discriminate the even parity states ($|uu\rangle$ or $|dd\rangle$) from the odd-parity ones ($|ud\rangle$ or $|du\rangle$). It is not difficult to verify that when two photons have different spatial modes, they will both appear at the output port 1 or 2. If they have the same spatial modes, each output port 1 and 2 has one and only one photon. A photon emitting from output port 2 is measured in the diagonal basis of the two DOFs.

With these two parity check devices, we can concentrate partially hyperentangled N -photon GHZ states that are entangled in the polarization and the spatial modes simultaneously.

3. Hyperconcentration

The partially hyperentangled N -photon GHZ state can be written as

$$\begin{aligned} |\Psi\rangle_{AB\dots C} &= (\alpha|HH\dots H\rangle + \beta|VV\dots V\rangle) \\ &\otimes (\delta|a_u b_u \dots c_u\rangle + \eta|a_d b_d \dots c_d\rangle). \end{aligned} \quad (7)$$

The parameters satisfy the normalization conditions $|\alpha|^2 + |\beta|^2 = 1$ and $|\delta|^2 + |\eta|^2 = 1$. The subscripts A, B, \dots, C represent the photons belonging to Alice, Bob, ..., Charlie and x_u and x_d are the two potential spatial modes of photon X ($X = A, B, \dots, C$). These N parties can be spatially far apart. The purpose of the hyperconcentration scheme is to obtain a maximally entangled state in both DOFs, i.e., the maximally hyperentangled GHZ state

$$\begin{aligned} |\Phi\rangle_{AB\dots C} &= \frac{1}{\sqrt{2}}(|HH\dots H\rangle + |VV\dots V\rangle) \\ &\otimes \frac{1}{\sqrt{2}}(|a_u b_u \dots c_u\rangle + |a_d b_d \dots c_d\rangle). \end{aligned} \quad (8)$$

To achieve this, we use two identical less-entangled states to distill maximal hyperentanglement probabilistically. We start with two states $|\Psi\rangle_{A_1 B_1 \dots C_1}$ and $|\Psi\rangle_{A_2 B_2 \dots C_2}$.

First, we convert the second state to

$$\begin{aligned} |\Psi\rangle_{A_2 B_2 \dots C_2} &= (\alpha|VV\dots V\rangle + \beta|HH\dots H\rangle) \\ &\otimes (\delta|a_{2d} b_{2d} \dots c_{2d}\rangle + \eta|a_{2u} b_{2u} \dots c_{2u}\rangle). \end{aligned} \quad (9)$$

The flip of polarization state can be realized by half wave plates oriented at 45° . And the flip of spatial mode can be simply realized by changing their names. The initial state of the $2N$ -photon system can be written as

$$\begin{aligned} &|\Xi\rangle_{A_1 B_1 \dots C_1 A_2 B_2 \dots C_2} \\ &= [\alpha^2|HH\dots HVV\dots V\rangle + \beta^2|VV\dots VHH\dots H\rangle \\ &\quad + \alpha\beta(|HH\dots HHH\dots H\rangle + |VV\dots VVV\dots V\rangle)] \\ &\otimes [\delta^2|a_{1u} b_{1u} \dots c_{1u} a_{2d} b_{2d} \dots c_{2d}\rangle + \eta^2|a_{1d} b_{1d} \dots c_{1d} a_{2u} b_{2u} \dots c_{2u}\rangle \\ &\quad + \delta\eta(|a_{1u} b_{1u} \dots c_{1u} a_{2u} b_{2u} \dots c_{2u}\rangle + |a_{1d} b_{1d} \dots c_{1d} a_{2d} b_{2d} \dots c_{2d}\rangle)]. \end{aligned} \quad (10)$$

The schematic for hyperconcentration is shown in Fig.3. Firstly, one party, say Alice puts her qubits A_1 and A_2 into the polarization parity check device while the second party Bob guides his qubit B_1 and B_2 into the spatial mode parity check device. Both of them select the even-parity terms by requiring that both the two output ports 1 and 2 have one and exactly one photon. Then the selected state can be written as

$$\begin{aligned} &|\Xi'\rangle_{A_1 B_1 \dots C_1 A_2 B_2 \dots C_2} \\ &= \alpha\beta\delta\eta(|HH\dots HHH\dots H\rangle + |VV\dots VVV\dots V\rangle) \\ &\otimes (|a_{1u} b_{1u} \dots c_{1u} a_{2u} b_{2u} \dots c_{2u}\rangle + |a_{1d} b_{1d} \dots c_{1d} a_{2d} b_{2d} \dots c_{2d}\rangle). \end{aligned} \quad (11)$$

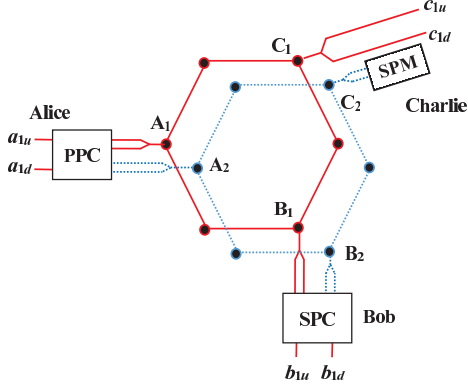


Figure 3. Schematic diagram of the proposed hyperconcentration protocol. Maximal hyperentanglement is distilled from two identical less-entangled N -photon GHZ states (solid and dotted) distributed among N parties who are spatially separated. Each party has a photon from each of the two less-entangled N -photon states. One party (Alice) applies a PPC to check the polarization parity of A_1 and A_2 and another party (Bob) uses SPC to check the spatial mode parity of B_1 and B_2 . For the other $N - 2$ parties (Charlie, etc), single-photon two-qubit measurements (SPM) can be performed on their second photons. For certain measurement results of A_2 and B_2 , the quantum system collapses to the maximally hyperentangled GHZ state.

The probability of getting this state is $4|\alpha\beta\delta\eta|^2$. After Alice and Bob's measurement on particle A_2 and B_2 , the collapsed $(2N - 2)$ -photon state can be written as

$$\begin{aligned}
 & |\Xi''\rangle_{A_1 B_1 \dots C_1 \dots C_2} \\
 &= \frac{1}{2}(|HH\dots H\rangle + (-1)^p |VV\dots V\rangle) \\
 &\otimes (|a_{1u} b_{1u} \dots c_{1u} \dots c_{2u}\rangle + (-1)^q |a_{1d} b_{1d} \dots c_{1d} \dots c_{2d}\rangle)
 \end{aligned} \tag{12}$$

Here the parameters p and q depend on Alice and Bob's measurement results. If the polarization measurement results are $|+\rangle_{A_2} |+\rangle_{B_2}$ or $|-\rangle_{A_2} |-\rangle_{B_2}$, $p = 0$. Otherwise, $p = 1$. And if the spatial mode measurement results are both d or u , $q = 0$. Otherwise, $q = 1$. To get the desired maximally hyperentangled N -photon state, each of the other parties performs a single-photon two-qubit measurement (SPM) on his/her second photon. The SPM setup is shown in Fig.4.

Then the final state is

$$\begin{aligned}
 & |\Xi'''\rangle_{A_1 B_1 \dots C_1} \\
 &= \frac{1}{2}(|HH\dots H\rangle + (-1)^P |VV\dots V\rangle) \\
 &\otimes (|a_{1u} b_{1u} \dots c_{1u}\rangle + (-1)^Q |a_{1d} b_{1d} \dots c_{1d}\rangle)
 \end{aligned} \tag{13}$$

Here P and Q depend on all the N parties' measurement outcomes. If the number of $|-\rangle$ is even (odd), $P = 0$ (1). And when the number of d is even (odd), $Q = 0$ (1). Then one party can perform the phase-flip operation $\sigma_z = |H\rangle\langle H| - |V\rangle\langle V|$ ($\sigma_z = |x_1\rangle\langle x_1| - |x_2\rangle\langle x_2|$) when $P = 1$ ($Q = 1$) to obtain the desired state $|\Phi\rangle_{A_1 B_1 C_1}$. Thus, the N parties can share the maximally hyperentangled state with a total success

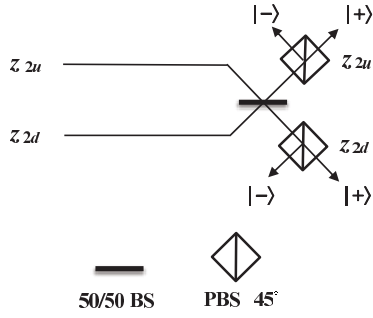


Figure 4. Schematic diagram of the single-photon two-qubit measurement. Both the two DOFs of the single photon are measured in the diagonal basis. The measurement of the spatial mode is realized by the BS and of the polarization state by the PBS at 45° .

probability of $4|\alpha\beta\delta\eta|^2$, which is the same as the hyperconcentration scheme for the two-photon state [45]. The relation between the success probability and the parameters of the initial states is shown in Fig.5.

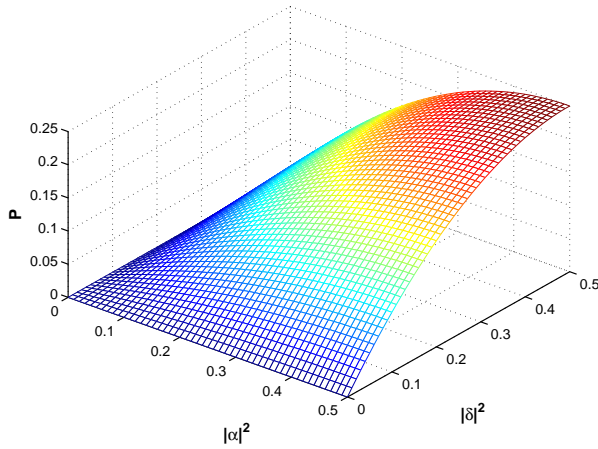


Figure 5. The success probability of the hyperconcentration scheme as a function of the coefficients of the initial state.

4. Discussion and Summary

We have proposed a hyperconcentration scheme for N -photon partially hyperentangled GHZ states. Each of the N parties holds two photons, which come from two identical less-entangled states. One party performs the polarization parity check measurement while another performs the spatial mode parity check measurement. The other $N - 2$ parties are only required to perform single-photon two-qubit measurements in the diagonal basis on both the two DOFs. By selecting the even-parity states in both the two parity check measurements, the remote N parties can share the maximally hyperentangled GHZ state with a certain probability. The total success probability

depends on the parameters of the initial states, with the maximum success probability being 25%. The success probability is not optimal. This is due to the fact that maximal entanglement in both DOFs should be achieved. Since we restricted ourselves to linear optics, parity checks are based on the measurement of photons, after which, the photons are destroyed. If nonlinear interactions which can realize quantum nondemolition (QND) measurements are utilized, failed instances can be reused iteratively and the success probability of hyperconcentration schemes can be improved [46, 47]. Fortunately, the success probability in our scheme does not decrease with the growth of photon number. The success probability for the N -photon state is the same as that of the two-photon scheme [45].

There is another method for entanglement concentration called as the parameter splitting method [45], which also only requires linear optical elements. The common point of this method and ours is that both of them are practical and can be realized with current technology. Compared with our scheme, the parameter splitting method has a higher success probability. However, it requires the parameter information which is unknown in our protocol. The information can be obtained by measuring some samples. Therefore, which method is a better choice depends on the amount of states to be concentrated.

In our scheme, only two parties perform the parity check. However, it can be changed to N parity checks, among which at least one PPC and one SPC are required. The success probability is the same since after the success of the first PPC and the first SPC the remaining parity check measurements will definitely give the even-parity results.

The success of our hyperconcentration scheme is based on the two parity check measurements. In principle, one and only one detector clicks in each parity check measurement, which is the signal of success. However, according to Eq.(5), there exists the probability that two photons arrive at the same detector, which may causes an error if the detectors cannot distinguish between one and two photons. One solution is using the photon number resolving (PNR) detector. However, it is expensive and uncommon. Another solution to eliminate this error is using an improved parity check devices. For the polarization parity check, two PBSs are introduced so that two photons with different polarizations will trigger two separate detectors. The improved PPC is shown in Fig.6. For the spatial mode parity check, additional BSs before the PBS at 45° can reduce the probability of errors. Imperfect optical elements and detectors will nevertheless decrease the success probability and cause errors in practice. In this case, postselection is required to solve these problems by strictly selecting the case in which each output port 1 and 2 has one and only one photon.

In our scheme, since the parameters are unknown, two less-entangled states are employed to distill one maximal hyperentangled GHZ state probabilistically. When N is large, this method consumes $2N$ photons to obtain an N -photon state probabilistically. A more practical approach would be to obtain information about the unknown

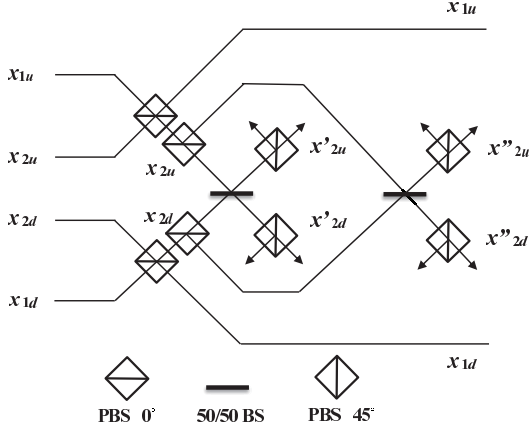


Figure 6. Schematic diagram of the improved polarization parity check device. Two PBSs at 0° were added to avoid the situation that two photons go to the same detector.

parameters by measuring a sufficient number of sample states. Then given the known parameters, an additional quantum state can be produced to assist the concentration. The auxiliary state required is

$$|\varphi\rangle_{A_2B_2} = (\alpha|VV\rangle + \beta|HH\rangle) \otimes (\delta|a_{2d}b_{2d}\rangle + \eta|a_{2u}b_{2u}\rangle) \quad (14)$$

The principle is shown in Fig.7. Alice and Bob perform PPC and SPC on A_1, A_2 and B_1, B_2 , respectively. By keeping the even-parity state in both these two DOFs, the N parties share the maximal hyperentangled state. The success probability is also $4|\alpha\beta\delta\eta|^2$. However, this method requires that the two parties Alice and Bob be located at the same place.

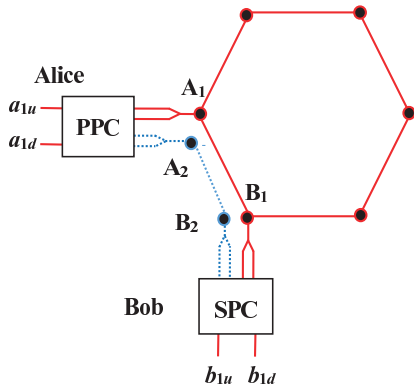


Figure 7. Schematic diagram of the hyperconcentration protocol assisted by two auxiliary photons. Alice performs a polarization parity check on A_1 and A_2 while SPC is used to check the spatial mode parity of B_1 and B_2 . By selecting on the even-parity states in both these two DOFs, the quantum system collapses to the maximally hyperentangled GHZ state.

To sum up, we have presented a hyperconcentration scheme for an N -photon hyperentangled state based on one polarization parity check measurement and one

spatial mode parity check measurement, which only require linear optical elements. And for the remaining $N - 2$ parities, only single-qubit measurements are required. This method can help remote parties share the maximally hyperentangled GHZ state which can be used in subsequent quantum information processing. The success probability is the same as that of the two-photon hyperconcentration scheme. These features can make our protocol more useful for practical applications in long-distance quantum communication.

Acknowledgement

XL is supported by the National Natural Science Foundation of China under Grant No. 11004258 and the Fundamental Research Funds for the Central Universities under Grant No.CQDXWL-2012-014. SG acknowledges support from the Ontario Ministry of Research and Innovation and the Natural Sciences and Engineering Research Council of Canada.

Reference

- [1] Ekert A K 1991 Phys. Rev. Lett. 67 661
- [2] Bennett C H, Brassard G and Mermin N D 1992 Phys. Rev. Lett. 68 557
- [3] Deng F G and Long G L 2003 Phys. Rev. A 68 042315
- [4] Nielsen M A and Chuang I L 2000 Quantum Computation and Quantum Information (Cambridge: Cambridge University Press)
- [5] Bennett C H and Wiesner S J 1992 Phys. Rev. Lett. 69 2881
- [6] Bennett C H, Brassard G, Crepeau C, Jozsa R, Peres A and Wootters W K 1993 Phys. Rev. Lett. 70 1895
- [7] Long G L and Liu X S 2002 Phys. Rev. A 65 032302
- [8] Deng F G, Long G L and Liu X S 2003 Phys. Rev. A 68 042317
- [9] Wang C, Deng F G, Liu X S and Long G L 2005 Phys. Rev. A 71 044305
- [10] Briegel H J, Dür W, Cirac J I and Zoller P 1998 Phys. Rev. Lett. 81 5932
- [11] Kwiat P G 1997 J. Mod. Opt. 44 2173
- [12] Barreiro J T, Langford N K, Peters N A and Kwiat P G 2005 Phys. Rev. Lett. 95 260501
- [13] Vallone G, Ceccarelli R, Martini F De and Mataloni P 2009 Phys. Rev. A 79 R030301
- [14] Barreiro J T, Wei T C and Kwiat P G 2008 Nature Phys. 4 282
- [15] Walborn S P, Almeida M P, Souto Ribeiro P H, Monken C H 2006 Quan. Inf. Com. 6 336
- [16] Ren B C and Deng F G 2014 Sci. Rep. 4 4623
- [17] Ren B C, Wei H R and Deng F G 2013 Laser Phys. Lett. 10 095202
- [18] Sheng Y B, Deng F G and Long G L 2010 Phys. Rev. A 82 032318
- [19] Ren B C, Wei H R, Hua M, Li T and Deng F G 2012 Opt. Express 20 24664
- [20] Simon C and Pan J W 2002 Phys. Rev. Lett. 89 257901
- [21] Sheng Y B, Deng F G and Zhou H Y 2008 Phys. Rev. A 77 062325
- [22] Sheng Y B and Deng F G 2010 Phys. Rev. A 81 032307
- [23] Li X H 2010 Phys. Rev. A 82 044304
- [24] Sheng Y B and Deng F G 2010 Phys. Rev. A 82 044305
- [25] Deng F G 2011 Phys. Rev. A 83 062316
- [26] Kwiat P G and Weinfurter H 1998 Phys. Rev. A 58 R2623
- [27] Walborn S P, Padua S and Monken C H 2003 Phys. Rev. A 68 042313
- [28] Schuck C, Huber G, Kurtsiefer C and Weinfurter H 2006 Phys. Rev. Lett. 96 190501

- [29] Barbieri M, Vallone G, Mataloni P and De Martini F 2007 Phys. Rev. A 75 042317
- [30] Ren X F, Guo G P and Guo G C 2005 Phys. Lett. A 343 8
- [31] Song S Y, Cao Y, Sheng Y B and Long G L 2013 Quan. Inf. Proc. 12 381
- [32] Bennett C H, Bernstein H J, Popescu S and Schumacher B 1996 Phys. Rev. A 53 2046
- [33] Bose S, Vedral V and Knight P L 1999 Phys. Rev. A 60 194
- [34] Shi B S, Jiang Y K and Guo G C 2000 Phys. Rev. A 62 054301
- [35] Yamamoto T, Koashi M and Imoto N 2001 Phys. Rev. A 64 012304
- [36] Zhao Z, Pan J W and Zhan M S 2001 Phys. Rev. A 64 014301
- [37] Sheng Y B, Deng F G and Zhou H Y 2008 Phys. Rev. A 77 062325
- [38] Sheng Y B, Zhou L, Zhao S M and Zheng B Y 2012 Phys. Rev. A 85 012307
- [39] Deng F G 2012 Phys. Rev. A 85 022311
- [40] Sheng Y B, Deng F G and Zhou H Y 2010 Quan. Inform. Comput. 10 0272
- [41] Yildiz A 2010 Phys. Rev. A 82 012317
- [42] Sheng Y B, Zhou L and Zhao S M 2012 Phys. Rev. A 85 042302
- [43] Gu B 2012 J. Opt. Soc. Am. B 29 1685
- [44] Sheng Y B, Zhou L 2013 Entropy 15 1776
- [45] Ren B C, Du F F and Deng F G 2013 Phys. Rev. A 88 012302
- [46] Ren B C and Deng F G 2013 Laser Phys. Lett. 10 115201
- [47] Li X H, Chen X and Zeng Z 2013 J. Opt. Soc. Am. B 30 2774
- [48] Ren B C and Long G L 2014 Opt. Express 22 6547